Supporting Information

For

Lone-Pair Electron Driven Thermoelectrics at Room Temperature

Saikat Mukhopadhyay[1*], Thomas L. Reinecke[2*]

[1] *NRC Research Associate at Naval Research Laboratory, Washington, DC 20375*
[2] *Naval Research Laboratory, Washington, DC 20375*

[*]Correspondence should be made to: SM:saikatrel@gmail.com, TLR:tom.reinecke@nrl.navy.mil

Stability: The structures and the corresponding phase diagrams of Tl_3TaSe_4, Tl_3VS_4, In_3TaSe_4 and In_3VS_4 were predicted using Materials Project[1]. While Tl_3TaSe_4 and Tl_3VS_4 give stable ternary phase diagrams (as shown in Fig. S1), In_3TaSe_4 and In_3VS_4 are found to be thermodynamically unstable at 0K.

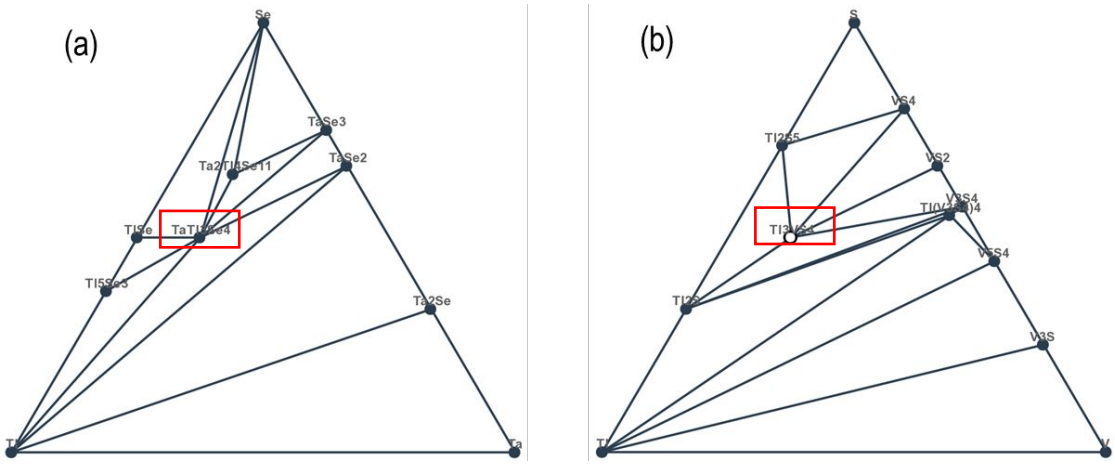

Figure S1: Phase diagrams for (a) Tl_3TaSe_4 and (b) Tl_3VS_4 from Materials Project [1].

Mean Square Displacement (MSD): Atomic displacement (u) of the j^{th} atom in the l^{th} unit cell along Cartesian axis α at a given time t can be written as[2]:

$$u^{\alpha}(jl,t) = \left(\frac{\hbar}{2Nm_j}\right)^{1/2} \sum_{\boldsymbol{q},\nu} \left[\omega_{\upsilon}(\boldsymbol{q})^{-1/2} \left[\hat{a}_{\nu}(\boldsymbol{q}) e^{(-i\omega_{\upsilon}(\boldsymbol{q})t)} + \hat{a}_{\nu}{}^{\dagger}(-\boldsymbol{q}) e^{(i\omega_{\upsilon}(\boldsymbol{q})t)}\right] e^{(i\boldsymbol{q}.\boldsymbol{r}(jl))} e_{\nu}^{\alpha}(j,\boldsymbol{q})\right]$$

where m is the atomic mass, N is the number of unit cells, $\boldsymbol{q}$ is the wave vector, ν is the branch index, $e_{\nu}^{\alpha}(j,\boldsymbol{q})$ is the polarization vector of the j^{th} atom in the l^{th} unit cell in mode ν, $\boldsymbol{r}(jl)$ is the atomic position and $\omega_{\nu}(\boldsymbol{q})$ is the phonon frequency. $\hat{a}_{\nu}$ and $\hat{a}_{\nu}{}^{\dagger}$ are phonon creation and annihilation operators. The expectation value of the squared atomic displacement is calculated as:

$$\left\langle |u^{\alpha}(jl,t)|^2 \right\rangle = \frac{\hbar}{2Nm_j} \sum_{\boldsymbol{q},\nu} \omega_{\nu}(\boldsymbol{q})^{-1} (1 + 2n_{\nu}(\boldsymbol{q},T)) |e_{\nu}^{\alpha}(j,\boldsymbol{q})|^2$$

where the phonon population $n_{\nu}(\boldsymbol{q},T)$ is:

$$n_{\nu}(\boldsymbol{q},T) = \frac{1}{e^{\left(\hbar\omega_{\nu}(\boldsymbol{q})/k_B T\right)} - 1}$$

The mean square displacements (MSD) were projected along the (111) direction as implemented in Phonopy[3]:

$$MSD = \frac{\hbar}{2Nm_j} \sum_{\boldsymbol{q},\nu} \omega_{\nu}(\boldsymbol{q})^{-1} (1 + 2n_{\nu}(\boldsymbol{q},T)) |n.e_{\nu}^{\alpha}(j,\boldsymbol{q})|^2$$

We projected the MSDs along (111)-direction (Fig. S2) using a $31 \times 31 \times 31$ mesh-points, which were chosen based on rigorous convergence tests.

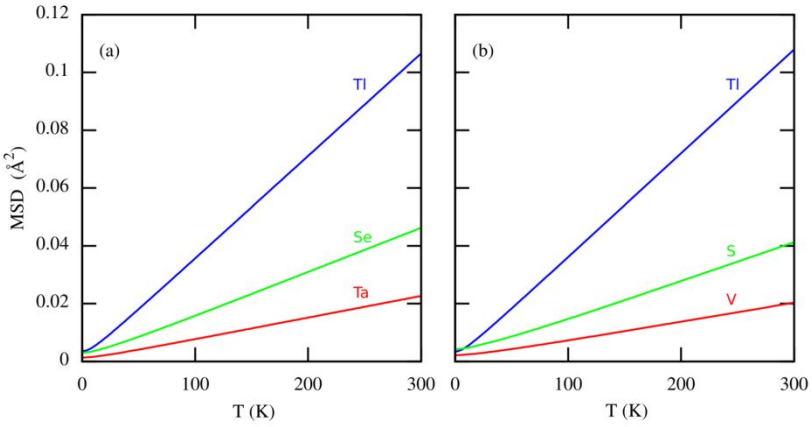

Figure S2: Mean square displacements of individual atoms for (a) Tl_3TaSe_4 and (b) Tl_3VS_4 at 300K.

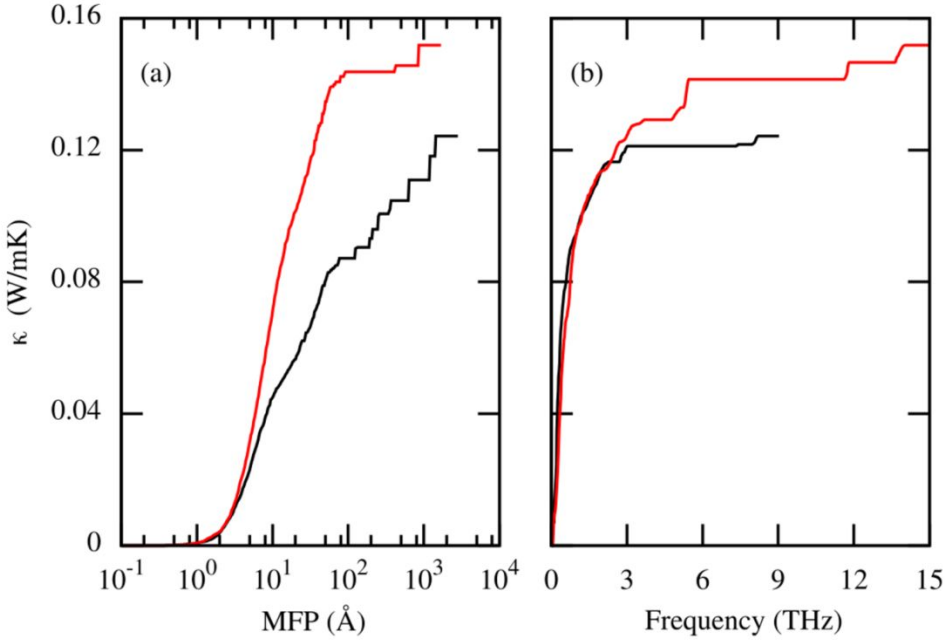

Figure S3: Accumulated κ for Tl_3TaSe_4 (black) and Tl_3VS_4 (red) at 300K as a function of (a) mean free path (MFP) and (b) phonon frequency.

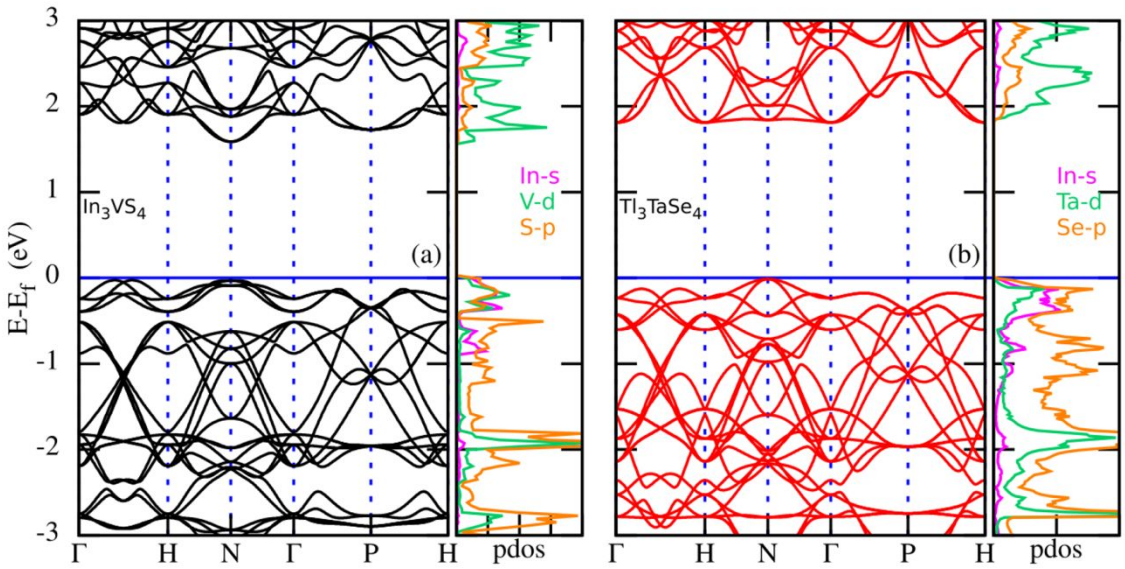

Figure S4: Electronic band structure and density of states projected on orbitals for (a) In_3VS_4 and (b)In_3TaSe_4. The blue horizontal lines are the Fermi levels of the corresponding compounds.

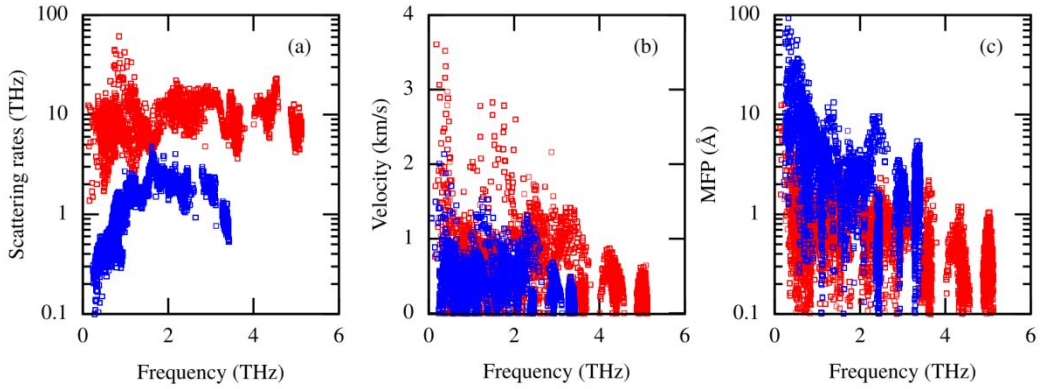

Figure S5: Comparison of lattice dynamical properties of In_3VS_4 (red) and Tl_3VSe_4 (blue): (a) scattering rates, (b) group velocity and (c) mean free path.

Thermal conductivity: Higher scattering rates in In_3XY_4 than those in Tl_3XY_4 (as shown in Fig. S4) give lower κ (<0.1 W/mK) In_3XY_4. This was verified by calculating κ from almaBTE[4] and Phono3py[5] which give similar κ.

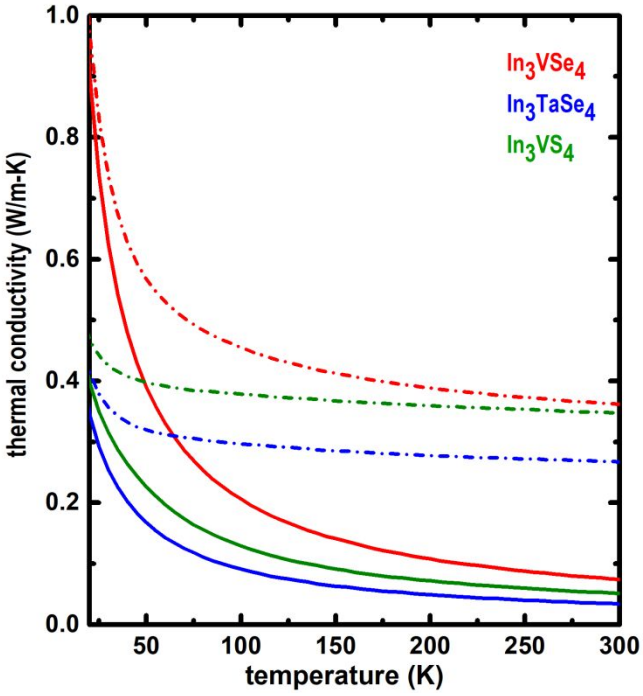

Figure S6: Thermal conductivity for In_3VSe_4 (red), In_3TaSe_4 (blue) and In_3VS_4 (green). The solid lines are κ- contributions from the phonon Boltzmann equation[4,5] and the dashed are κ from the two channel model [6].

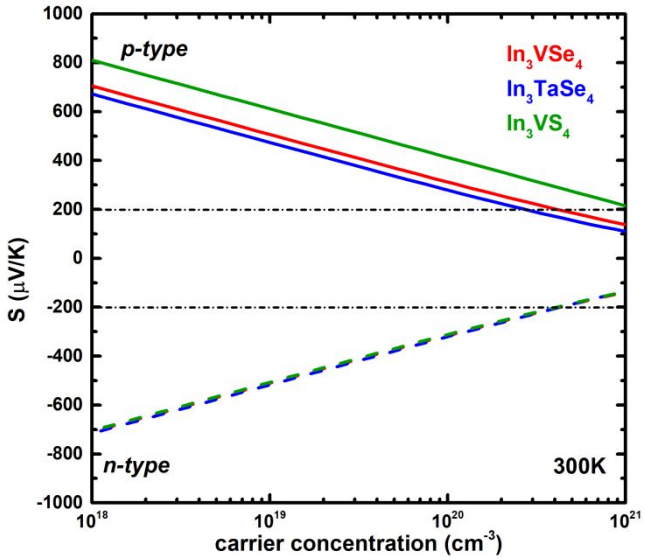

Figure S7: Calculated Seebeck coefficient of In_3VSe_4, In_3TaSe_4 and In_3VS_4 as a function of carrier concentration at 300K.

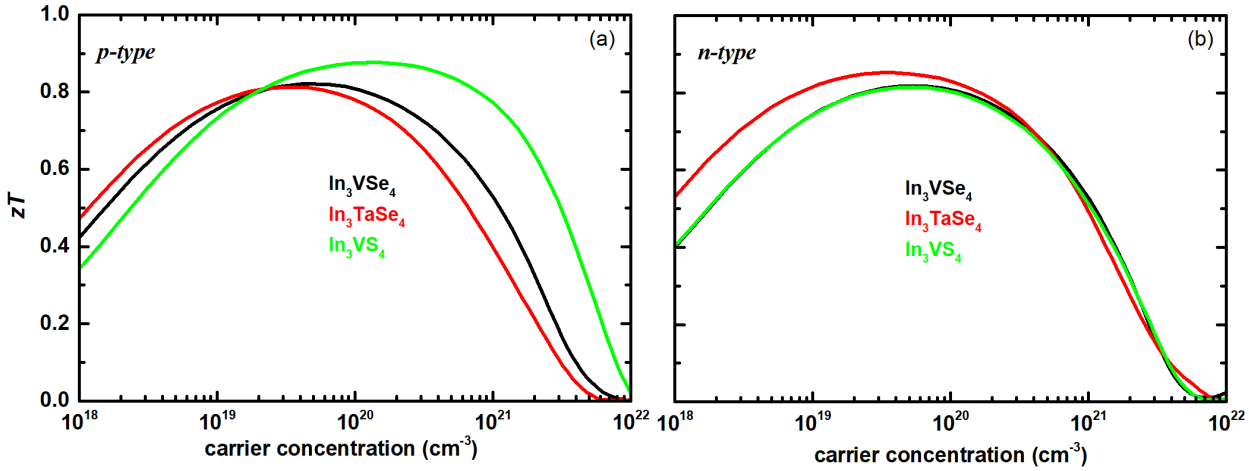

Figure S8: Thermoelectric properties of In_3VSe_4, In_3TaSe_4 and In_3VS_4 as a function of carrier concentration at 300K when doped (a) p-type and (b) n-type. A relaxation time; $\tau = 9 \times 10^{-14}s$ was used for all the cases to be consistent with Tl_3XY_4 discussed in the main text.

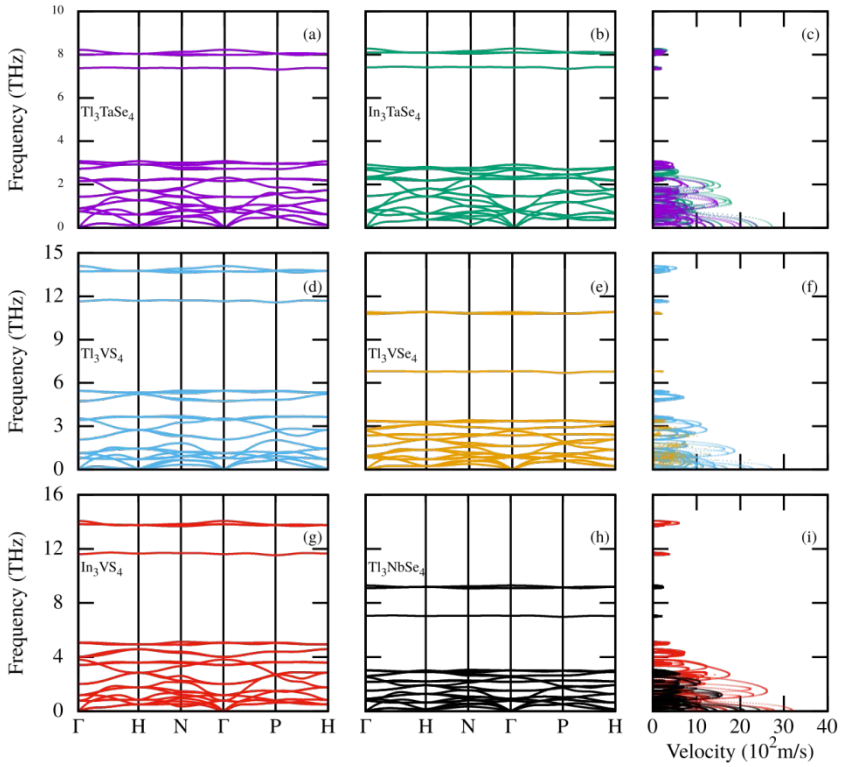

Figure S9: Comparative lattice dynamical properties in Z_3XY_4 (X=In/Tl, X=Ta/V/Nb and Y= S/Se) as a result of variation of Z (a-c), Y (d-f) and X ,Y, Z (g-i) atoms

References

(1) Jain, A.; Ong, S. P.; Hautier, G.; Chen, W.; Richards, W. D.; Dacek, S.; Cholia, S.; Gunter, D.; Skinner, D.; Ceder, G.; Persson, K. A., Commentary: The Materials Project: A Materials Genome Approach to Accelerating Materials Innovation, *APL Materials*. **2013**, *1*, 011002 (1-11) .

(2) Wallace, D. C. *Thermodynamics of Crystal*. (Dover Publications, 1998).

(3) Togo, A.; Tanaka, I., First Principles Phonon Calculations in Materials Science, *Scr. Mater.* **2015**, *108*, (1-5).

(4) Carrete, J.; Vermeersch, B.; Katre, A.; van Roekeghem, A.; Wang, T.; Madsen, G. K. H.;

Mingo, N., almaBTE : A Solver of the Space–Time Dependent Boltzmann Transport Equation for Phonons in Structured Materials, *Comput. Phys. Commun.* **2017**, *220, (351-362)*

(5) Togo, A., Chaput, L. & Tanaka, I. Distributions of Phonon Lifetimes in Brillouin Zones. *Phys. Rev. B.* **2015**, ***91***, 094306 (1-31).

(6) Mukhopadhyay, S.; Parker, D. S.; Sales, B. C.; Puretzky, A. A.; McGuire, M. A.; Lindsay, L., Two-Channel Model for Ultralow Thermal Conductivity of Crystalline Tl_3VSe_4., *Science.* **2018**, *360, (1455-1458).*